J Neurophysiol 89: 212–228, 2003.
10.1152/jn.00016.2002.

Systematic Changes in Motor Cortex Cell Activity With Arm Posture During Directional Isometric Force Generation

LAUREN E. SERGIO AND JOHN F. KALASKA
Centre de Recherche en Sciences Neurologiques, Département de Physiologie, Université de Montréal, Montreal, Quebec H3C 3J7, Canada

Submitted 10 January 2002; accepted in final form 6 September 2002

Sergio, Lauren E., and John F. Kalaska. Systematic changes in motor cortex cell activity with arm posture during directional isometric force generation. *J Neurophysiol* 89: 212–228, 2003. 10.1152/jn.00016.2002. We report here the activity of 96 cells in primate primary motor cortex (MI) during exertion of isometric forces at the hand in constant spatial directions, while the hand was at five to nine different spatial locations on a plane. The discharge of nearly all cells varied significantly with both hand location and the direction of isometric force before and during force-ramp generation as well as during static force-hold. In addition, nearly all cells displayed changes in the variation of their activity with force direction at different hand locations. This change in relationship was often expressed in part as a change in the cell's directional tuning at different hand locations. Cell directional tuning tended to shift systematically with hand location even though the direction of static force output at the hand remained constant. These directional effects were less pronounced before the onset of force output than after force onset. Cells also often showed planar modulations of discharge level with hand location. Sixteen proximal arm muscles showed similar effects, reflecting how hand location-dependent biomechanical factors altered their task-related activity. These findings indicate that MI single-cell activity does not covary exclusively with the level and direction of net force output at the hand and provides further evidence that MI contributes to the transformation between extrinsic and intrinsic representations of motor output during isometric force production.

INTRODUCTION

The muscle activity pattern required to produce a desired whole-arm reaching movement or a net isometric force at the hand varies with the posture of the arm. This results from posture-dependent changes in muscle contractile properties and in their pulling angles and moment arms at the joint(s) across which they act (Buchanan et al. 1986; Buneo et al. 1997; Flanders and Soechting 1990; Hoffman and Strick 1999; Karst and Hasan 1991a,b; Van Zuylen et al. 1988; Wadman et al. 1980; Winters and Woo 1990) as well as from posture-dependent variations of global mechanical properties of the limb (Flash and Mussa-Ivaldi 1990; Gordon et al. 1994; Mussa-Ivaldi et al. 1985; Shadmehr and Mussa-Ivaldi 1994).

The nature of the representation of arm motor output variables in the primary motor cortex (MI) is the subject of continuing lively debate (Ajemian et al. 2000; Ashe 1997; Cabel et al. 2001; Johnson et al. 2001; Kakei et al. 1999; Moran and Schwartz 1999a,b; Scott and Kalaska 1997; Scott et al. 2001; Taira et al. 1996; Todorov 2000). If MI single-cell activity covaries explicitly and exclusively with global extrinsic or hand-centered parameters of motor output, all of the putative transformations necessary to generate muscle activation signals must occur elsewhere. Alternatively, if MI single-cell activity was modulated by arm posture, it could be implicated in the transformation of the representation of motor output variables from external to internal coordinate frameworks. Adding to the debate is evidence that the representation can change with time during motor tasks (Johnson et al. 2001; Shen and Alexander 1997a,b; Zhang et al. 1997).

Signals covarying closely with extrinsic parameters of arm movement can be extracted from MI discharge at both single-cell and population levels (Caminiti et al. 1990, 1991; Georgopoulos et al. 1983, 1988; Johnson et al. 2001; Kalaska et al. 1989; Moran and Schwartz 1999a,b; Schwartz 1992; Schwartz et al. 1988). However, other studies have shown that the activity of wrist-related MI cells is altered by changes in the posture of the wrist during movement (Kakei et al. 1999) and during isometric-force tasks (Fromm 1983).

Similarly, MI single-cell discharge is also modulated by arm geometry during whole-arm reaching movements along parallel hand paths in different locations in a three-dimensional (3D) space (Caminiti et al. 1990, 1991) and while making reaching movements along the same two-dimensional (2D) planar hand paths but with the arm in two different orientations (Scott and Kalaska 1997; Scott et al. 1997). Both studies reported arm geometry-dependent changes in directional tuning of single cells. However, unlike Caminiti et al. (1990, 1991), Scott and Kalaska (1997) found no evidence of a systematic shift in the distribution of directional preferences of the cells between the two arm orientations. This discrepancy was attributed to the differing geometries of the tasks in the two studies (Scott and Kalaska 1997). Specifically, rotation of the arm posture about an axis parallel to the plane of motion of the hand might not result in a net shift in the overall distribution of observed 2D cell directional tuning curves, even if the global tuning functions of single cells are coupled to and rotated with changes in arm geometry (Scott and Kalaska 1997). One can predict that a systematic rotation of MI directional tuning functions

Address for reprint requests: J. F. Kalaska, Département de Physiologie, Université de Montréal, C.P. 6128, Succ. Centre-ville, Montreal, Quebec H3C 3J7, Canada (E-mail: kalaskaj@physio.umontreal.ca).

The costs of publication of this article were defrayed in part by the payment of page charges. The article must therefore be hereby marked "*advertisement*" in accordance with 18 U.S.C. Section 1734 solely to indicate this fact.

would be observed in a 2D task that involved rotation of arm postures about an axis perpendicular to the plane of motor output at the hand. It is also important to assess to what degree this rotation is seen prior to and after the onset of overt motor output, i.e., prior to and after the arrival of peripheral reafferent signals.

Therefore we studied MI single-cell activity while monkeys exerted isometric output forces at the hand in eight constant spatial directions in the horizontal plane against a rigid force transducer that was positioned in nine different spatial locations in a horizontal plane. This required rotations of arm posture about the vertical axis through the shoulder joint. The isometric-force task also avoided confounds introduced by the complex dynamics of whole-arm movement. As predicted, directional tuning rotated systematically with arm posture at both single-cell and population levels. Preliminary results have been reported previously during static force generation (Kalaska et al. 1997, 1998; Sergio and Kalaska 1997a,b). Here we present evidence that similar effects can be seen during the force-ramp epoch and during the behavioral reaction time prior to the onset of force generation. We also present further evidence that this effect reflects mechanical anisotropies in the mechanical properties of the arm.

METHODS

Task apparatus

Two juvenile male rhesus monkeys (*Macacca mulatta*, 5 and 6 kg) exerted isometric forces with their whole arm against a rigid manipulandum that they held in their hand. The manipulandum was a 20-mm ball on the end of a 65-mm vertical rod attached to a 6 df force transducer (Gamma F3/T10 system, Assurance Technologies). The transducer was housed inside a box that could be clamped into one of nine different locations in front of the animal (Fig. 1*A*, squares). The central location was at the midline, 20 cm in front of the monkeys' sternum, approximately level to the zyphoid process. The other eight locations were equally spaced every 45° on a circle of 8 cm radius, starting at 0° to the right (Fig. 1*A*).

The manipulandum rod passed freely through a small hole in a thin metal plate that was attached by hinges to the top of the transducer housing on the edge furthest away from the monkey. The free end of the plate closest to the monkey sat on a micro-switch. If the monkey rested its hand on the plate or otherwise applied forces to it, the switch would close and halt the task. In this way, all forces generated at the hand were applied only to the manipulandum.

A cursor on a monitor positioned at eye level 60 cm in front of the monkey gave continuous visual feedback about the current force generated by the monkey at its hand in the *x-y* (horizontal) plane (Fig. 1*A*). The *x* axis was aligned to the 0–180° (right-left) direction in front

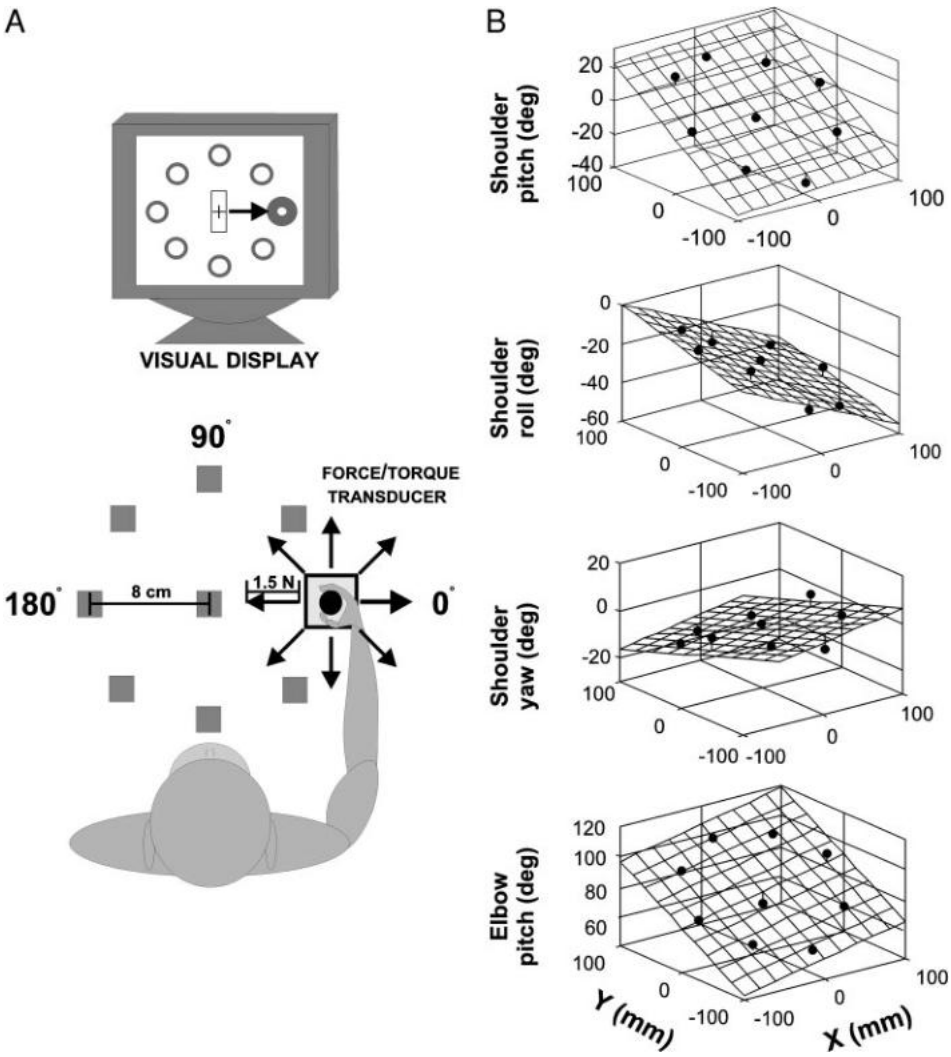

FIG. 1. *A*: experimental setup and task apparatus used in the study. Circles on the monitor illustrate the locations of the peripheral isometric force targets. In the task, only 1 target circle was visible at any one time. Squares in front of animal represent locations on a horizontal plane at which the force transducer was placed. Monkeys grasped the handle of the force transducer and generated force at the hand to displace the cursor on the monitor. The location of the monitor and target locations remained invariant for the different hand locations. *B*: static shoulder and elbow angles for each hand location in the workspace. Joint angles follow the convention used by Soechting et al. (1989). Zero degrees for each orientation are as follows: shoulder pitch—upper arm vertical, positive pitch is a forward rotation; shoulder roll—forearm in a parasagittal plane, positive roll is an outward rotation; shoulder yaw—upper arm in a parasagittal plane, positive yaw is an outward rotation; elbow pitch—lower arm fully flexed, positive pitch is elbow extension (angle between upper and lower arms). The oblique grid is the best-fit plane of the 8 points in each figure.

of the monkey, and the y axis to the 90–270° direction. Force data were sampled and stored every 5 ms.

The spatial position of the limb joints was recorded (OptoTrak 3020, Northern Digital) in one animal at each of the nine transducer locations to calculate limb segment orientations using standard rigid body reconstruction techniques (Fig. 1*B*) (see Soechting and Flanders 1989 for a description of the coordinate frame).

Behavioral task

To start each trial, a circle representing a central force target appeared at the center of the monitor. The diameter of the circle corresponded to a force range of 0.20 N. A constant programmed bias in the display of cursor position required the monkey to exert a force of +0.3 N at 90° along the *y* axis away from its body to position the cursor at the center of the central target (Fig. 2). The monkey kept the cursor within the central target for a variable time period (2,000 ± 500 ms, Gaussian distribution). At the end of the central hold time, the central target disappeared and one of eight peripheral force targets arrayed in a circle around the central target appeared (Fig. 1*A*, circles; diameter: 0.28 N). The separation of the centers of the central and peripheral targets corresponded to a force change of 1.5 N. The monkey generated the 1.5 N force ramp in the indicated direction in the horizontal plane to move the cursor into the peripheral target and held it there for 2,000 ms to receive a liquid reward (Fig. 2). Note how the animals generated a smooth force ramp and did not relax the bias force before directing a force toward the peripheral target. Peripheral target directions were spaced at 45° intervals, starting from 0° to the right and proceeding counterclockwise (Fig. 1*A*). A complete data file comprised five successful replications of the isometric ramp-and-hold force outputs to the eight peripheral targets, presented in a randomized-block sequence, while the transducer was clamped at one hand location.

The monkey performed sequential files of trials with the manipulandum clamped in different workspace locations. Locations were tested in a pseudo-random sequence for a total of nine files (360 successful trials) per complete data set. In this way, the animal viewed the same display and produced output forces at the hand in the same eight constant directions in hand-centered spatial coordinates while holding the hand at up to nine different spatial locations.

The monkeys also received continual visual feedback about the forces generated at the hand in the vertical (*z*) axis. A rectangular box was drawn about the cursor (Fig. 1*A*) and moved with it on the monitor as the monkey generated forces in the horizontal plane. The vertical position of this box relative to the cursor was continuously adjusted as a function of the measured vertical forces. A small constant vertical offset in the display of the box required the monkey to apply a 0.3-N downward force in the *z* axis to center the cursor in the box. This allowed the monkeys to rest their hand gently on the manipulandum while performing the task. The vertical length of the box was scaled as a function of the acceptable range of vertical forces (±0.26 N for *monkey A*, ±0.40 N for *monkey B*) about the constant vertical offset. If the *z* axis forces exceeded that range, the box shifted to a point where the cursor was no longer inside it, and the trial was terminated. In this way, the net output force vectors generated by the monkeys at the hand were confined to a narrow vertical range about the horizontal plane. This extra behavioral control prevented the monkeys from developing a strategy of systematically varying the *z* axis component of the net output force vectors at the hand as a function of target force direction or hand location in the workspace, which would confound the interpretation of cell activity.

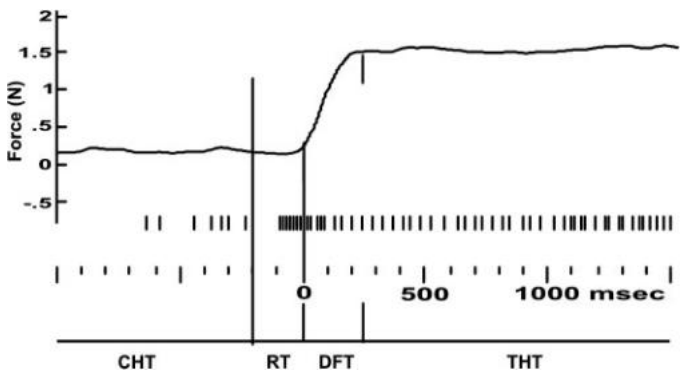

FIG. 2. Isometric force profile (solid line) and single-cell discharge (horizontal row of vertical lines) for 1 trial showing epochs analyzed in this study. Second and third vertical lines, the onset and end of dynamic force time. First vertical line, the appearance of the peripheral target on the monitor. The time scale is aligned to the onset of the isometric force ramp aimed at the peripheral target.

Data collection

The animals were trained to >80% success rates at all nine locations. They were then prepared for recording by implantation of a recording cylinder over MI using standard aseptic surgical techniques (Kalaska et al. 1989).

Conventional techniques were used to record the activity of single cells in MI (Kalaska et al. 1989). During each recording session, a microelectrode was advanced through the cortex while the animal performed the task at the central workspace location. When a cell was isolated, its task-related responses were tested initially by performing a few trials at several hand locations. The passive responses of cells were studied by manipulating the arm joints, brushing the skin and palpating muscles. The arm was monitored for signs of movements or muscle contractions during low-threshold intracortical microstimulation (ICMS) of the cortex. If a cell responded to active or passive movements of the contralateral shoulder and/or elbow but not to more distal joints and displayed directional tuning in at least one hand location, it was then subjected to further study in the task.

Attempts were made to record cells from all cortical layers. However, because the task required data collection for long time periods to test across all hand locations, there was a bias toward collecting complete data sets more frequently from large cells in intermediate layers.

The time needed to collect a complete data set also raises the possibility that changes in a cell's activity across data files might be due to temporal variations in cell responsiveness independent of the experimentally manipulated parameter of hand location (Kalaska et al. 1989; Scott and Kalaska 1997). This potential confound was handled in two ways. First, files were collected from different locations in a pseudorandom sequence for each cell to minimize the risk of confounding systematic changes in activity due to hand location with systematic temporal changes. Second, a repeated data file was periodically recorded from the first hand location tested. If it appeared to be comparable to the data from the original file at that location, the cell's activity was considered stable. If changes were evident, data files were also replicated from other hand locations until consistent results were obtained. If repeatable results were never achieved, all data files for that cell were deleted. This rarely happened.

Activity was recorded from 16 proximal-arm muscles in *monkey A* in separate recording sessions. Muscles were implanted percutaneously with pairs of Teflon-insulated 50-μm single-stranded stainless steel wires. Implantations were verified by passing current through the wires to evoke focal muscular contractions (<1.0 mA, 30 Hz, 300-ms train). Multi-unit electromyographic (EMG) activity was amplified, band-pass filtered (100–3,000 Hz), half-wave rectified, integrated (5-ms time bins), and digitized on-line at 200 Hz. The muscles studied included the biceps brachii (2 sets), brachialis (1), anterior deltoid (1), medial deltoid (2), posterior deltoid (2), dorsoepitrochlearis (1), infraspinatus (2), latissimus dorsi (2), pectoralis (2), subscapularis (2), supraspinatus (1), teres major (2), rostral trapezius (2), caudal trapezius (2), triceps longus (2), and triceps medialis (1). These recordings

were done to assess the general effects of arm posture on EMG activity in this task to provide a benchmark against which to compare cell activity. They were not designed as a definitive biomechanical study of the properties of each muscle.

Near the end of recordings in each cylinder, small electrolytic lesions were made (5–10 μA, 5 s) in selected penetrations. At the conclusion of the experiment, the monkeys were deeply anesthetized with barbiturates and perfused with buffered saline and formalin. Pins were inserted into the cortex at known grid coordinates to delimit the area from which cell recordings were made, and the cortex was sectioned to permit localization of the marked penetrations.

Data analysis

BEHAVIORAL DATA. Successful performance of a trial involved three phases of force production (Fig. 2). First, exertion of a small static bias force in the horizontal plane directed away from the monkey positioned the cursor in the central target. Second, following peripheral target presentation, dynamic horizontal force ramps in different directions displaced the cursor into the target windows. Third, static horizontal forces in different directions kept the cursor at the peripheral targets. A number of sequential behavioral epochs were defined in each trial (Fig. 2). Center hold time (CHT) began when the animal placed the cursor in the central target and ended on peripheral target appearance. A mean ($\pm$SD) baseline force vector was calculated from the 100 force samples collected during the last 500 ms of the CHT. Reaction time (RT) was the interval between target appearance and the time at which there was a significant change in force applied to the transducer. This was defined as the 5-ms sample interval at which the horizontal force vector length deviated 2 SDs from the baseline force and remained so for three more consecutive 5-ms sample intervals. This marked the end of RT and the beginning of the dynamic-force time (DFT), which ended when the cursor first reached a stable force level in the peripheral target window (Fig. 2). This was defined as the time at which the rate of horizontal force change (the 1st derivative of the force level) was within 2 SDs of the mean rate of force change calculated during the last 1,500 ms of the trial. Peripheral target hold time (THT, Fig. 2) was the time from the end of the DFT to the end of the trial.

The time profile of the net output force exerted at the hand can be represented as a force trajectory in a 3D hand-centered force space. Ideally, the force trajectories should not change when the monkey performed the task at different hand locations. This was evaluated by statistical tests applied to the force output during the static and dynamic trial phases separately. These tests were done on the force data collected for only those cells recorded at all nine hand locations. Because there were four instances in which two cells were isolated and recorded simultaneously, there were 57 force data sets for the 61 cells studied at all nine hand locations.

To test for significant differences in force output during the static force production phases (CHT, RT, THT), the mean *x*, *y*, and *z* force components were subjected to a standard two-way ANOVA (main factors: hand location, force direction). To test for significant differences during the dynamic force phase (DFT), the data from each file were tested using a functional ANOVA (fANOVA) (Ramsey and Silverman 1997). This modified ANOVA treats the dependent variable (force) as a function of time and applies appropriate corrections to treat the forces as time-series data. For this analysis, the *x*, *y*, and *z* components of the force ramps during DFT for the five trials in a given target direction at a given hand location were each divided into 20 equal segments in force space and averaged. This was repeated for all eight force directions at each hand location. The fANOVA tested for differences in the 20-segment sequences of the *x*, *y*, and *z* components of the mean force ramp for each target direction separately across all hand locations.

NEURAL DATA. Cell activity was subjected to a number of different analyses. First, an unbalanced repeated-measures ANOVA (program 5V, BMDP Statistical Software) determined if force direction or hand location had a significant main effect on the mean cell discharge rate during each behavioral epoch. Cells showing a significant statistical interaction between force direction and hand location were identified as evidence that the covariation of cell discharge level with force direction was modulated as a function of the location of the hand in the workspace.

An interaction between force direction and hand location on a cell's discharge could express itself in at least two different but nonexclusive ways (Scott and Kalaska 1997). The cell's directional tuning could change at different hand locations independent of any discharge rate changes. Alternatively, the directional tuning of the cell could remain constant, but the range of changes in cell discharge as a function of force direction (directional dynamic range) could vary across hand locations. Several analyses were performed to evaluate both possible effects.

To evaluate the force direction-related directional tuning, the preferred direction (PD) of each cell was calculated separately in each trial epoch at each hand location (Mardia 1972). The statistical significance of each directional tuning curve was tested using bootstrapping methods to assess whether the degree of directional bias of the tuning curve could have occurred by chance (Georgopoulos et al. 1988; Scott and Kalaska 1997; Sergio and Kalaska 1997a).

For all cases of significant directional tuning in a given epoch at both the central and a given peripheral location, the change in PD between the two locations was calculated. To determine whether this PD shift was significant, a second bootstrapping procedure was used. This second procedure assessed whether the difference in PDs between the two hand locations could have occurred by chance. It was based on the assumption that if the tuning function of a cell is the same in two hand locations, then the distribution of differences of the bootstrapped estimates of cell PD at each location will be normally distributed and centered on a 0° difference. This test was implemented as follows. First, we generated a bootstrapped estimate of the directional tuning curve of the cell at the peripheral hand location by random selection with replacement of five measures of the discharge rate of the cell from the sample of five single trials at each of the eight directions, separately. From these 40 sampled trials, a bootstrapped estimate of the PD (PD_b) was calculated by standard methods. This was repeated for the data at the central location. The difference in direction between the bootstrapped central and peripheral PD_b (ΔPD_b) was then calculated. This was repeated 1,000 times to generate a distribution of 1,000 bootstrapped ΔPD_b values, which were then rank ordered. The high and low limits of the 95% confidence interval (CI) were defined as the 25th and 975th largest ΔPD_b values (2-tailed test). A cell was considered to have undergone a significant shift in PD at a given peripheral hand location compared with that at the center if it was significantly directionally tuned at both the central and peripheral locations in that epoch and the value of 0° for ΔPD_b fell outside of the 95% CI of the distribution of bootstrapped ΔPD_b (i.e., the null hypothesis that the mean value for $\Delta PD_b = 0°$ can be rejected at $P < 0.05$, 2-tailed test).

The distribution of PD shifts from the central PD was calculated for all cells meeting the first condition in the preceding text (significant directional tuning at both the central and a given peripheral location) at each peripheral location. Two tests were performed on those PD shift distributions. A one-way ANOVA tested for any difference in the distributions of PD shifts across all peripheral hand locations. This assessed the directional behavior of the entire sample of cells that happened to be directionally tuned at both the central and given peripheral locations. Second, at each peripheral location, a paired *t*-test was used to determine if the mean PD shift was significantly different from 0°; that is, whether there was a significant directional bias in the distribution of PD shifts at a given location. Both tests were also applied to the distributions of significant single-cell PD shifts only (2nd condition in the preceding text). This latter analysis assessed the behavior specifically of only those cells in which there was

a significant directional shift between central and given peripheral hand locations.

The effect of hand location on the size of the force direction-related variation of a single cell's activity was tested in the following manner. The force-direction dynamic range (DR) was defined as the difference between the largest and smallest mean discharge rate associated with different directions of force during a given trial epoch (RT, DFT, THT) at a single hand location. A DR was calculated separately for each hand location, and the following index was calculated

$$(DR_P - DR_C)/(DR_P + DR_C) \quad (1)$$

where DR_C and DR_P are the force direction-related dynamic range measured at the central and a given peripheral location, respectively. The index will be positive or negative, depending on whether or not the force direction-related dynamic range increased or decreased at a peripheral location relative to that at the center, and zero if there was no change in dynamic range. The distribution of the values of DR indices for the sample of cells at each peripheral location was used to determine whether or not there was a systematic effect of hand location on the range of force direction-related changes in activity. A comparable analysis was performed on the grand mean discharge rate of each cell across all eight force directions in each epoch to determine whether hand location had a systematic effect on the overall level of task-related activity. That is, we tested whether or not there was a systematic spatial bias on the nature of the main effect of hand location on overall discharge rate across the entire sample of cells.

The effect of hand location on the overall level of activity of single cells was tested further using a multiple linear regression analysis. For this analysis, the variation of cell activity as a function of force direction was disregarded and the dependent variable was the grand mean cell activity level averaged across all 40 trials in the data file at each hand location during a given trial epoch. Regressions were performed on the variation of grand mean cell discharge as a function of *x*-*y* hand location, using the following equation

$$\hat{d} = a + b_1 \cdot X\_\text{location} + b_2 \cdot Y\_\text{location} \quad (2)$$

Because two independent variables were used, cell activity was regressed onto a best-fit plane. To test if the fitted regression plane was significantly nonhorizontal, an *F* test was performed on the regression coefficients (regress function, MATLAB, The Mathworks).

Cells showing a significantly nonhorizontal regression plane were examined further. To test for a uniform distribution of the workspace orientations of the regression planes across cells, a χ^2 test was performed on the computed *x* and *y* regression coefficients separately. A positive regression coefficient for the *y* axis would result in a plane tilted toward the animal, whereas a positive coefficient for the *x* axis would result in a plane tilted to the left of the animal.

The planar regression analysis was applied to only the 61 cells with data collected from all nine hand locations. Tests using the 61 cells showed that random removal of the data from different hand locations (equivalent to not recording a data file at that location) systematically reduced the values of regression coefficients and the frequency of cells with significant nonhorizontal regression planes, compared with the results obtained with the complete data sets.

The EMG activity recorded from proximal-arm muscles was subjected to the same analyses as the cells. Whenever analyses required the pooling of results from cells or muscles, all data collected while the monkeys performed the task with the left arm were subjected to a mirror-image transformation about the 90–270° (*y*) axis.

RESULTS

Data base

The task-related activity was recorded from 179 cells during 151 penetrations in MI of three hemispheres from two juvenile monkeys (108 and 32 cells from the left and right hemispheres of *monkey A* and 39 cells from the right hemisphere of *monkey B*). Of these cells, 61 were successfully studied in all nine hand locations (48 and 13 in *monkeys A* and *B*, respectively). In an additional 35 cells (25 and 10 from *monkeys A* and *B*), data were collected from only five to eight hand locations (the center plus at least the 4 cardinal or diagonal hand locations). The remaining 83 cells were studied at fewer than five hand locations and will not be described here. Most of the cells were recorded from caudal MI (Fig. 3) (Crammond and Kalaska 1996, 2000).

Isometric forces

The mean behavioral reaction time across all trials for both animals was 240 ms, and the mean dynamic force time was 313 ms.

The mean force profiles generated at the hand were similar at all nine hand locations (Fig. 4) despite a large variation in the limb segment orientation angles (Fig. 1*B*). The nine force profiles for each of the eight force directions start and end at nearly the same location in force space and are confined to a narrow range in the vertical axis (Fig. 4*A*). Note the lack of initial hooks in the force profiles, indicating that the monkeys did not release the bias force before generating a force in the target direction. Few data sets showed a main effect of hand location on the *x*, *y*, or *z* components of the force outputs during CHT, RT, and THT (Table 1). Some 14–19% of the force traces showed a main effect of target direction during RT. In principle, the RT is a static force period that ends with the onset of the force ramps. The directional effects seen here are likely a threshold phenomenon, reflecting the small directional force-vector deviations necessary to detect the end of the RT epoch (see METHODS, Fig. 2). In contrast, during the THT epoch, while the animals maintained static forces in the peripheral targets, all data sets showed a main effect of target direction on the *x* and *y* force components, whereas only one showed a main effect on the *z* component (Table 1). Across epochs, few force data showed a location-direction interaction with one exception—17 sets showed an interaction during THT for the *y* axis force component only (Table 1). Also noteworthy is the scarcity of significant effects on the *z* axis force components in all three static epochs.

These ANOVAs used the mean force outputs averaged over periods of hundreds of ms. Such an analysis is inappropriate for the DFT epoch, during which the forces change rapidly. A

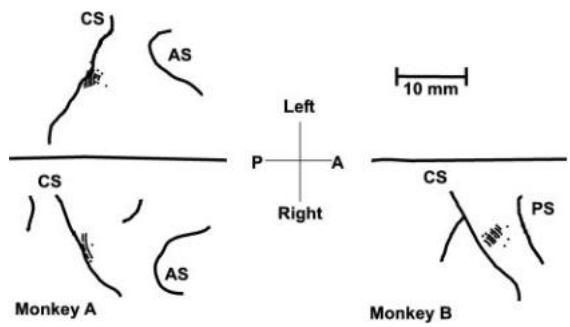

FIG. 3. Drawing of the cortical surface of both monkeys (right hemisphere only for *monkey B*) showing the electrode penetration sites. P, posterior; A, anterior; CS, central sulcus; AS, arcuate sulcus; PS, precentral sulcus.

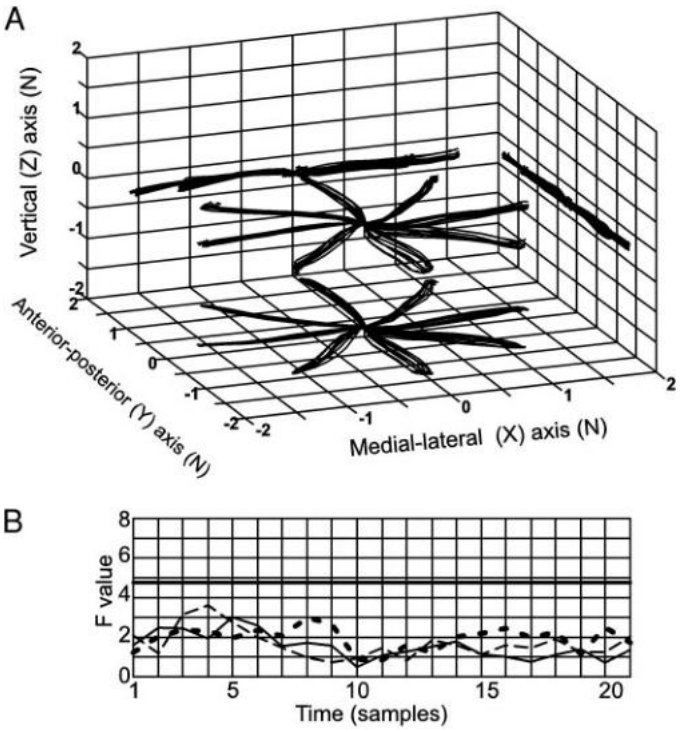

FIG. 4. *A*: mean force trajectories for *monkey A* during dynamic-force time (DFT). The 9 lines in each direction are the mean of all trials at each hand location for that force direction. *B*: result of functional ANOVA (fANOVA) analysis for 1 cell in 1 force direction across all hand locations. The thick horizontal line indicates the critical *F* value for significance at the 0.05 level. Thick dashed line: *x*-axis component of force, solid line: *y*-axis component, thin dashed line: *z*-axis component.

modified ANOVA intended for time-series data, fANOVA, was applied to the DFT data (see METHODS). A total of 1,368 tests were performed (57 data sets, 8 target directions, 3 force vector components). Figure 4*B* displays the *F* value as a function of time for one data set in one target direction and indicates no significant change across hand locations. For *monkey A*, only five data sets showed a significant difference in the *x* component of the force output for target direction 270°. These deviations lasted for periods of from 3 to 10 of the 20 force-profile segments in different sets. This typically represents a 48- to 160-ms-long deviation in force output for this one target direction. There were no other significant differences for any other data set or in any other target direction for this animal ($P < 0.05$), nor for any force data in *monkey B*. Because only 5/1368 tests displayed a significant difference (0.36%), the animals did not appear to display any systematic differences in their force outputs at the different hand locations during DFT.

These analyses confirmed that behavioral control of the forces generated by the monkeys, in particular in the vertical axis, had resulted in largely invariant force outputs in the horizontal plane at each location and had successfully eliminated nearly all location-related biases in the vertical component of the force output. Any systematic hand location-dependent variation in cell activity could not be readily explained by systematic changes in the net force output at the hand.

EMG activity: general observations

Muscle activity varied systematically with force direction and hand location (Fig. 5). In particular, muscle activity often displayed two major effects during force generation at different locations—large changes in the overall level of activity and changes in the force-direction tuning function of the muscle, including changes in its depth (dynamic range) and directionality (PD). For example, changes in EMG activity of the right infraspinatus muscle for isometric forces at different directions while the hand was at the 0° location (Fig. 5*A*) and the 180° location (Fig. 5*B*) resulted in a shift in PD between the two hand locations (Fig. 5*C*). The PD shifts across all locations followed an arc-like pattern about the mid-sagittal axis whereby the PD tended to rotate clockwise (CW) relative to that seen at the central location for positions on the right of the midline and counterclockwise (CCW) for positions on the left.

The effect of force direction and hand location were as strong during dynamic force generation as during static force maintenance. All muscle sets showed a significant main effect of both hand location and force direction and a significant interaction effect between location and direction during both DFT and THT (Table 2; Wald test, $P < 0.01$). During RT, in contrast, all sets showed a main effect of location, but somewhat fewer showed direction and interaction effects. Even prior to target appearance (CHT), 26 (96%) muscle sets showed a main effect of hand location due to systematic changes in tonic EMG activity while generating a constant output force of +0.3 N along the $+y$ axis (Fig. 5*C*, circles).

Neuronal activity: general observations

The activity displayed by single MI cells (Figs. 6 and 7) showed many parallels to that seen for muscles. Nearly all cells showed a significant main effect of force direction and hand location on discharge level during all three trial epochs (Table 2). Significant interactions between force direction and hand location were less prominent during RT (77%) than during DFT and THT (98%) (Table 2).

TABLE 1. *Effect of hand location and force direction on mean force output during static epochs*

Factor	Location			Direction			Interaction		
Force Component	*x*	*y*	*z*	*x*	*y*	*z*	*x*	*y*	*z*
Epoch									
CHT	2 (4)	6 (11)	2 (4)	2 (4)	2 (4)	1 (2)	1 (2)	2 (4)	4 (5)
RT	4 (7)	8 (14)	4 (7)	10 (18)	11 (19)	8 (14)	2 (2)	0 (0)	1 (2)
THT	3 (5)	1 (2)	0 (0)	57 (100)	57 (100)	1 (2)	2 (4)	17 (30)	1 (2)

Two-way ANOVA, $P < 0.01$. Table shows the number (and percentages) of data sets ($n = 57$) that showed a significant effect of each experimental factor. CHT, center hold time; RT, reaction time; THT, peripheral target hold time.

Changes in directional tuning of muscle activity with hand location

One cause of an interaction effect between force direction and hand location is a change in a muscle's directional tuning with arm posture (Scott and Kalaska 1997). The distribution of PD changes was calculated at each hand location for all instances in which a muscle was significantly directionally tuned at both that location and the central location (Table 3*A*, Fig. 8). There were significant differences (ANOVA, $P < .01$) in the distributions of PD shifts across the eight peripheral hand locations during DFT and THT but not during RT (Table 3*A*). A different question is whether the PD shift distribution at each location was directionally biased, that is, significantly skewed away from 0° mean PD shift. No directional bias was found at any location during RT (paired *t*-test, $P > 0.01$), eliminating the possibility that the nonsignificant ANOVA during RT resulted from a significant but uniform shift across all hand locations. In contrast, there was a significant CW shift of PDs at the 0° location and CCW shift at the 180° hand location during DFT, and significant CW rotations at both the 0 and 45° locations during THT ($P < 0.01$, Table 3*A*, Fig. 8).

TABLE 2. *Effect of hand location and force direction on MI cell and proximal arm muscle activity*

	Factor		
Epoch ↓	Location	Direction	Interaction
Motor cortical cells			
RT	92 (96)	92 (96)	74 (77)
DFT	94 (98)	96 (100)	94 (98)
THT	95 (99)	95 (99)	94 (98)
Proximal muscles			
RT	27 (100)	24 (89)	20 (74)
DFT	27 (100)	27 (100)	27 (100)
THT	27 (100)	27 (100)	27 (100)

Unbalanced repeated-measures ANOVA, Wald test $P < 0.01$. Table shows the number (and percentages) of data sets ($n = 96$ cells, 27 muscles) that showed a significant effect of each experimental factor. DFT, dynamic force time.

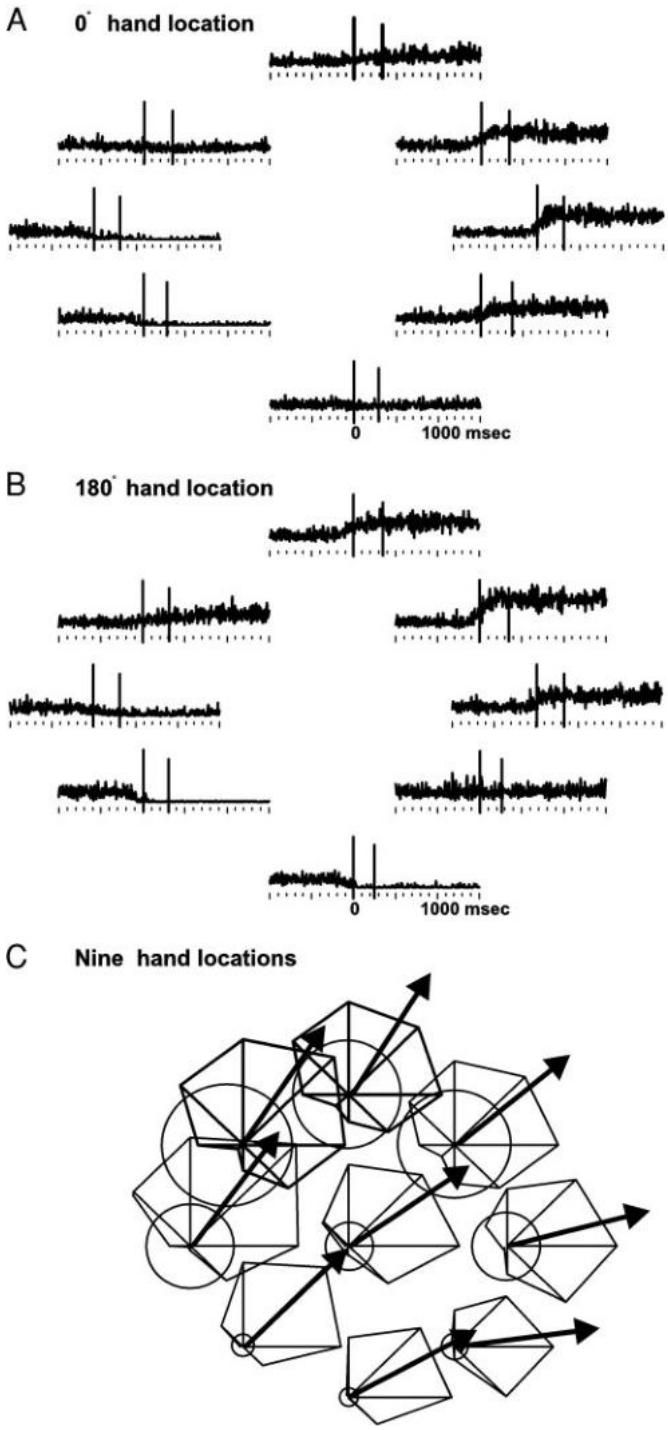

The effect of hand location was next evaluated for only the cases of significant PD shifts for single muscles between the central and peripheral locations as assessed by bootstrapping (see METHODS). Significant single-muscle PD shifts were common at several hand locations in the DFT and THT epochs but infrequent during RT (Table 3*B*, Fig. 8, ■). As was the case for the full sample, significant differences in the distributions of significant PD shifts were seen during DFT and THT but not RT (ANOVA, Table 3*B*). Significant CW shifts occurred at 0 and 45° and CCW shifts at 180 and 225° during both DFT and THT (*t*-test, Table 3*B*, Fig. 8).

These quantitative tests confirmed the general impression that hand location had a significant effect on the force direction-related tuning of muscles, and that this resulted in an arc-like rotation of PDs about the mid-sagittal axis. They also

FIG. 5. *A*: electromyographic (EMG) activity of the right infraspinatus muscle during isometric force production while the hand is at the rightward (0°) hand location. Each histogram illustrates the average activity from 5 trials in that force direction. Data are oriented to the onset of DFT (*time 0*, 1st solid vertical line). The 2nd vertical line denotes the average end of DFT and beginning of target hold time (THT) for the 5 trials at each force direction. *B*. EMG activity from the same muscle while the hand is held at the leftward (180°) hand location. *C*: polar-plot representations of the response of the same muscle at all nine hand locations. The position of each polar plot corresponds to the relative location of the hand on the planar work surface. The polar plots for the hand locations at 0° (*A*) and 180° (*B*) are reproduced on the right and left, respectively, and the upper-most polar plot corresponds to the hand location furthest away from the monkey's body (90°). The radius of the circle in the polar plot represents the mean muscle activity during the center hold (CHT) epoch. The length of each of the 8 axes in the polar plot represents the mean activity over the 5 trials of force production in each direction during the peripheral target hold (THT) epoch. The heavy arrow corresponds to the preferred direction of the muscle during THT. Note the rotation in the directional tuning of the muscle during THT and the change in mean muscle amplitude during CHT for the different hand locations.

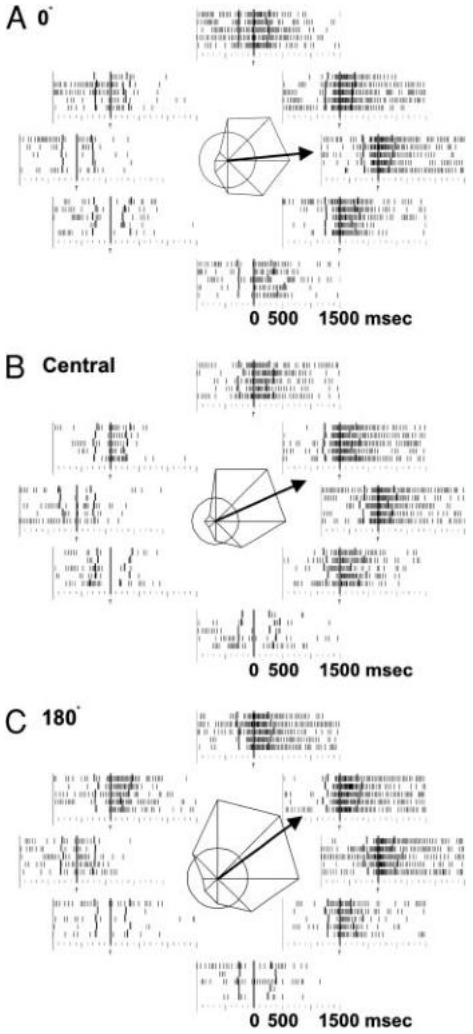

FIG. 6. Discharge pattern of a primary motor cortex cell during isometric force production while the hand was held at the rightward (*A*), central (*B*), and leftward (*C*) locations. The 8 rasters in each panel illustrate cell activity during 5 trials for 1 force direction, and each raster location corresponds to the direction of force production away from the starting central force target. Data are oriented to the onset of DFT denoted by a solid vertical line at *time 0*. For each trial, the heavy tick mark to the left of DFT onset shows the time of target onset while the heavy tick mark to the right shows the time at which the final static level of force within the peripheral force target was attained (start of THT). The 8 rasters surround a polar plot depiction of cell activity. The radius of the circle in the polar plot represents the mean cell discharge rate during the center hold (CHT) epoch. The length of each axis represents the mean discharge rate over the 5 trials in that direction during the peripheral target hold (THT) epoch. The heavy arrow corresponds to the preferred direction of the cell during THT.

revealed that the effects were equally strong during DFT and THT but less prominent prior to the onset of force generation (RT).

Changes in directional tuning of cells with hand location

Similar systematic patterns of directional tuning changes at different times during the trial were also found for many MI cells (Table 3, *A* and *B*, Fig. 9). Quantitative analysis of all instances of significant directional tuning at both the central location and individual peripheral locations revealed a significant difference in the distributions of PD shifts across the eight peripheral hand locations during DFT and THT but not RT (ANOVA, $P < 0.01$, Table 3*A*). A paired *t*-test revealed significant CW- and CCW-biased directional shifts at the rightward and leftward hand locations, respectively, especially during DFT and THT (Table 3*A*). The hand locations along the mid-sagittal plane (90 and 270°) did not show a significantly biased directional shift in any trial epoch.

The percentage of single cells displaying a significant PD change at a given hand location relative to that at the center increased from RT to DFT and THT (Table 3*B*, Fig. 9, ■). An ANOVA on only those cells revealed a significant difference in distributions across locations in all trial epochs, and paired *t*-tests showed systematic CW shifts to the right of the midline and CCW shifts to the left of the midline in all trial epochs (Table 3*B*, Fig. 9*B*, ■).

Quantitative analysis indicated a similarity in the directional shifts of muscles and cells. A two-way unbalanced ANOVA (main factors: hand location and source—cells or muscles) revealed a significant main effect ($P < 0.01$) for hand location but not for source during both DFT and THT.

Closer scrutiny of Fig. 9 revealed other trends. First, during THT, the frequency of significant single-cell PD shifts was fairly constant at all eight peripheral hand locations (Table 3*B;* Fig. 9*B*, ■). However, for locations to the right or left of midline, the distribution was strongly biased toward CW and CCW changes, respectively. In contrast, they were more symmetrically distributed at the two extremes of the distributions of PD shifts for the 90 and 270° locations. Second, the distributions of all PD shifts were usually unimodal with a single pronounced mode during THT (Fig. 9*B*) and DFT (data not shown). This was also the case for the PD shift distributions at 90 and 270° during RT (Fig. 9*A*). However, the distributions at the lateral hand locations usually showed two pronounced peaks during RT, one spanning 0° and one more eccentrically located (Fig. 9*A*) where the few instances of significant PD shifts in that epoch were concentrated. The eccentric peaks during RT corresponded to the single major peak at the same locations during THT and DFT. This suggested the transient presence of two functionally different sub-populations of directionally tuned cells during RT, one that showed a directional shift prior to force onset at a given hand location and one that did not. During (DFT) and after (THT) the isometric force ramps had been generated, a greater proportion of the cells showed posture-dependent PD changes.

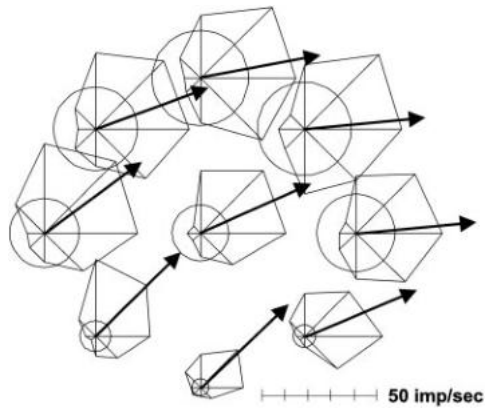

FIG. 7. Polar plot representations of the cell shown in Fig. 6 at all 9 hand locations. Display format is the same as for the EMG polar plots in Fig. 6.

TABLE 3A. *Mean angular changes, in degrees, of preferred direction between peripheral and central hand location for all directionally tuned cells/muscles*

	Peripheral Hand Location								
Epoch	0°	45°	90°	135°	180°	225°	270°	315°	Center
Motor cortical cells									
RT	−3.3 (80)	−5.1 (84)	−5.6 (75)	6.7 (77)	3 (82)	13.7 (78)†	5 (80)	−4.9 (79)	(82)
DFT*	−10.8 (90)†	−1.6 (91)	4.5 (85)	8.2 (93)	12.9 (92)†	18.5 (92)†	−2.5 (91)	−16.4 (88)	(94)
THT*	−11.4 (96)†	−10.5 (94)	4.4 (95)	14.3 (95)†	18.9 (99)†	11.3 (87)†	6.4 (93)	−10.6 (89)	(96)
Proximal muscles									
RT	−5.5 (64)	−4 (72)	−15.6 (64)	11.4 (64)	11.3 (76)	−6 (60)	2.1 (84)	−8.4 (76)	(84)
DFT*	−16.6 (92)†	−14.1 (92)	−7.6 (92)	3.2 (92)	12.7 (100)†	12.3 (100)	10.3 (100)	−6.7 (92)	(92)
THT*	−21.7 (92)†	−15.5 (92)†	−17.5 (96)	3.6 (100)	13.3 (100)	14.9 (100)	10.8 (100)	−6.8 (96)	(100)

Values in parentheses are the percent of total sample that are tuned at that location. Positive angle values denote counterclockwise rotation in preferred direction relative to the central hand location. Negative values denote clockwise rotations. * Distribution of mean angular changes are significantly different across hand locations (ANOVA, $P < 0.01$). † Significant directional shift across sample of all directionally tuned cells or muscles at a particular hand location (paired *t*-test, $P < 0.01$).

The activity during the early part of the RT epoch is a continuation of the CHT tonic discharge before the cells begin to respond to the target information. However, this is not likely to explain the weaker influence of arm posture on directional tuning during RT compared with later epochs. Several analyses were repeated using only the activity during the last 100 ms of the RT. The number of cells showing a main effect of location remained essentially constant, 89/96 rather than 92/96 (Table 2). The number of cells that were directionally tuned increased slightly, from 80% on average across hand locations (Table 3*A*) to 85%. Most importantly, there was little effect on the directional analysis. There was still no significant difference in the PD shift distributions of the whole sample (ANOVA, cf. Table 3*A*) nor a significant directional bias in the PD shifts (paired *t*-test, cf. Table 3*A*). Only 17–32% of the cells showed significant PD shifts between the central and peripheral locations (cf. Table 3*B*), there was a significant difference in the PD shift distributions of those cells across locations (ANOVA) and significant CW biases in the PD shift distributions at 0 and 315° (paired *t*-test).

One final observed effect of hand location was a loss of directional tuning. During RT, for instance, 82% of the cells were directionally tuned at the central location. Of those cells, 11–25% were not directionally tuned at one or another of the peripheral locations. This loss of directional tuning was less prominent during THT, when 96% of the cells were tuned at the central location and only 1–13% of those cells were not tuned at different peripheral locations.

These analyses were all based on the mean discharge rate during different epochs. Peak discharge rates were also determined on a trial-by-trial basis using a 50-ms sliding window incremented in 10-ms intervals from 200 ms before target onset to the end of the DFT. Similar overall trends were found for the effects of hand location on peak rates as for epoch means. For instance, 84% of the cells showed a significant main effect of hand location as opposed to 96–98% seen for the mean discharge in RT or DFT epochs (Table 2). This difference in incidence is likely due to the greater inter-trial variability of 50-ms peak rates than epoch means. Because there were no substantive differences, they will not be described further.

Regression analysis of muscle and cell activity with hand location

A linear regression was performed on muscle activity in each epoch to calculate a best-fit planar function for the grand mean of activity averaged across all force directions at each location against its *x-y* coordinates (Fig. 10*A*, see METHODS, *Eq. 2*). The incidence of significant nonhorizontal planar changes in grand mean activity level with hand location increased systematically from CHT to DFT/THT, and those planar func-

TABLE 3B. *Mean angular changes, in degrees, of preferred direction between peripheral and central hand location for only those cells/muscles with a significant directional shift between the central and peripheral hand location*

	Peripheral Hand Location							
Epoch	0°	45°	90°	135°	180°	225°	270°	315°
Motor cortical cells								
RT*	−27.6 (16)†	−21.4 (11)	−26.2 (15)	6.8 (18)	27.8 (10)†	35.6 (15)	35.6 (15)	−10.5 (22)
DFT*	−17.0 (54)†	−14.1 (39)	−6.6 (37)	15.8 (52)†	18.9 (52)†	15.6 (51)†	7.6 (33)	−22.2 (42)†
THT*	−21.2 (59)†	−10.1 (43)	−2.9 (49)	14.3 (51)†	25.7 (47)†	25.5 (47)†	10.8 (51)	−13.0 (52)†
Proximal muscles								
RT	−22.7 (4)	−20.6 (4)	16.7 (12)	−17.2 (16)	0.0 (0)	0.0 (0)	−20.0 (4)	19.8 (12)
DFT*	−18.8 (52)†	−27.4 (32)†	−3.8 (28)	9.8 (44)	16.6 (56)†	21.0 (60)†	14.4 (56)	−12.5 (48)
THT*	−21.1 (68)†	−17.4 (68)†	−22.6 (48)	10.2 (48)†	19.9 (52)†	20.9 (68)†	18.2 (60)	1.0 (44)

Values in parentheses are the percent total sample of cells/muscles displaying significantly different preferred direction compared to the central location. Positive angular values denote counterclockwise rotation in preferred direction relative to the central hand location. Negative values denote clockwise rotations. * Mean angular changes are significantly different across hand locations (ANOVA, $P < 0.01$). † Significant directional shift across sample of all single cells or muscles with a significant PD shift at that hand location (paired *t*-test, $P < 0.01$).

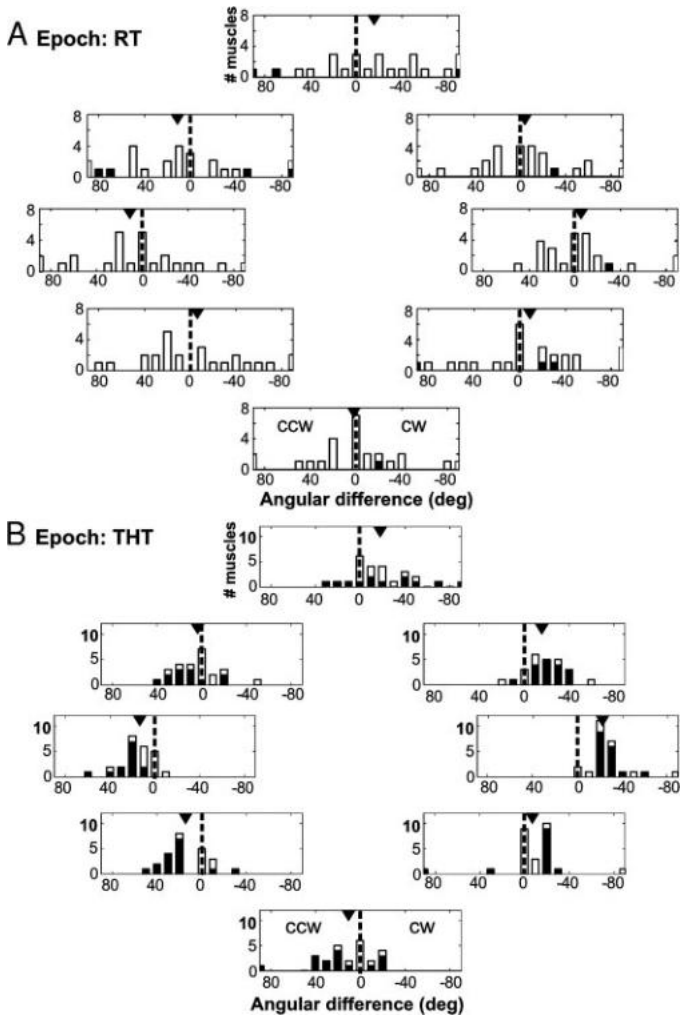

FIG. 8. Histograms (10° bins) displaying the distribution of shifts in directional tuning between central and peripheral hand locations for each muscle during RT (*A*) and THT (*B*). To be included, a muscle had to be significantly directionally tuned (bootstrap test) during the epoch at the central location and the particular peripheral location. The position of the histogram corresponds to the peripheral hand location. □, nonsignificant directional shifts at a given peripheral hand location (bootstrap test). ■, muscles showing a significant shift in their preferred direction (PD) relative to the central location at a given peripheral hand location. ▼, mean PD shift for the total distribution shown. CCW, counterclockwise; CW, clockwise.

tions accounted for 66–98% (mean: 80–82%) of the variance in the data across epochs (Figs. 10*A* and 11, ■; Table 4).

Comparable results were observed for the 61 cells recorded at all nine hand locations. The incidence of significant nonhorizontal planar functions for grand mean cell activity increased modestly from CHT to THT (Table 4). The significant planar functions accounted for between 63 and 98% (mean 81–84%) of the variance in the data across epochs (Figs. 10*B* and 11, ■; Table 4). Many of the 35 cells with data collected from only five to eight hand locations also showed significant planar regressions, but they were not included in Table 4 or Fig. 11 (see METHODS). The mean slopes for cells with significant nonhorizontal planes were between 0.06 and 0.09 imp · s^{-1} · mm^{-1} (range: 0.02–0.25) across epochs.

The planar regression analysis was repeated using the muscle or cell activity for each of the eight force directions separately. This had only a modest effect on results. For example, the percentage of cells that displayed a significant planar regression on hand location during THT ranged from 46 to 74% for different force directions, compared with 64% when the grand mean activity across all eight force directions at a given location was used.

Distribution of regression plane orientations

The orientation of each significantly nonhorizontal regression plane can be quantified by calculating the normal vector to the best-fit plane. For example, the best-fit plane for the muscle in Fig. 10*A* had a normal vector pointing toward the animal and to the right, whereas that for the cell in Fig. 10*B* was oriented toward the monkey and to the left.

Across the sample population, more planes were tilted toward the animal, as indicated in Fig. 12 by the greater number of normal vectors intersecting the spherical surface in front of the frontal plane axis ($P < 0.05$, χ^2 test). Those cells had positive regression coefficients along the *y* axis, indicating greater activity for hand locations further away from the animal (Fig. 11). Second, most cell regression-plane normal vectors were distributed in the lower right and upper left quadrants of the sphere, forming an elliptical distribution whose major axis deviated away from the body midline toward the arm being used (Fig. 12). The normal vectors for the cells collected when the monkeys performed the task with their left arm (Fig. 12, ○) were mirror-reflected about the mid-sagittal axis on the figure. As originally collected, those best-fit plane normal vectors were mainly in the upper right and lower left quadrants, opposite to that seen for the right arm (Fig. 12, ●). These trends were seen in all epochs and suggest that there was a mirror-image change about the body midline for the spatial orientation of the best-fit regression planes for cells in the two hemispheres. The best-fit planes of muscles showed similar trends (Fig. 12, ▲ and △).

The difference in grand mean cell activity between the central and each peripheral hand location was calculated for each cell in each epoch. A paired *t*-test ($P < 0.01$) tested the null hypothesis that the distributions of these differences were centered on zero at each hand location separately. Significant overall increases in the mean discharge level relative to that at the center were found for the three outer hand locations during CHT (45, 90, and 135°), and for four hand locations during THT (45, 90, 135, and 180°). No significant decreases were found. There were no systematic changes in overall cell discharge with hand location for the RT and DFT epochs.

Effect of hand location on dynamic range of cell activity

An interaction effect between direction and location could also be due to location-dependent changes in the depth of a cell's force-direction tuning curve. To test this possibility, we calculated dynamic range (DR) ratios (see METHODS, *Eq. 1*) for the whole cell sample during RT, DFT, and THT. There was no systematic difference in the distributions of DR ratios as a function of hand location in any epoch (ANOVA, $P > 0.01$). In addition, a paired *t*-test performed at each peripheral hand location found no systematic nonzero biases in the distributions of DR values ($P > 0.01$, RT, DFT, THT) between peripheral and central locations.

A planar regression of DR ratios with *x*-*y* hand location was

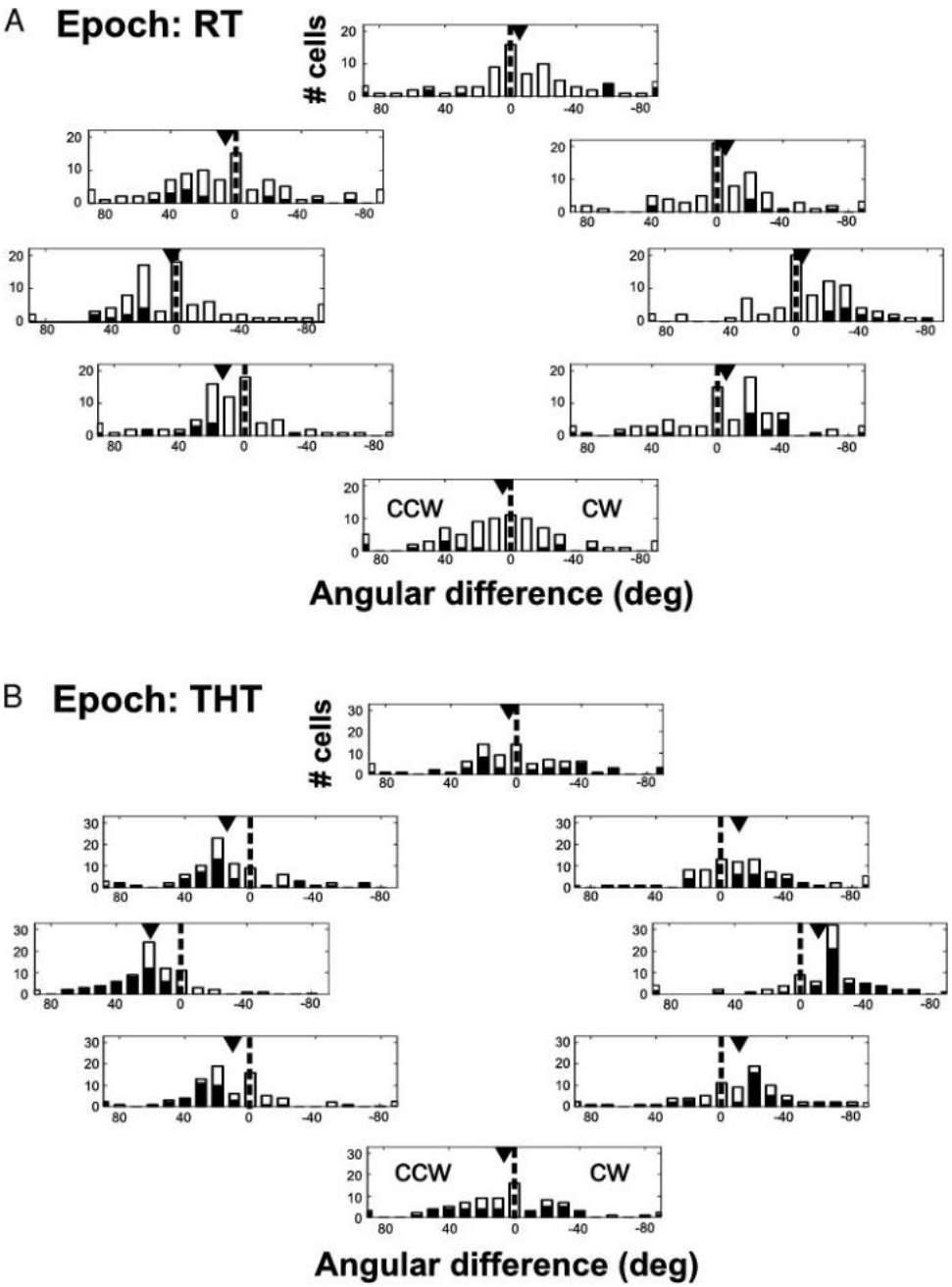

FIG. 9. Histograms displaying the distribution of shifts in directional tuning between central and peripheral hand locations for each cell during RT (*A*) and THT (*B*). Display format is the same as in Fig. 8. ▼, mean magnitude of PD shift for all cells in each histogram.

done on a cell-by-cell basis to further test for any systematic bias. As with the planar regressions on mean cell activity, only the 61 cells that were recorded in all nine hand locations were used for this analysis. A moderate number of cells had a hand location-dependent change in dynamic range that could be fit by a significantly nonhorizontal plane in the RT (20%), DFT (30%), and THT (18%) epochs.

The dynamic range also provides a measure of the relative strength of effect of force direction and hand location on cell activity levels. We calculated the distribution of direction-dependent DRs across all force directions at each hand location separately, and the location-dependent DRs across all hand locations for each force direction separately. The median value of the force direction-dependent DR ranged from 23.1 (DFT) to 13.1 imp/s (THT). In contrast, the median hand location-dependent DRs ranged from 22.8 (DFT) to 16.2 imp/s (THT). Values during the RT were intermediate.

DISCUSSION

At each hand location, MI cell activity was broadly tuned for net isometric force direction at the hand. This has been described previously for whole-arm isometric force generation (Georgopoulos et al. 1992; Taira et al. 1996) and while defending a given arm posture against loads applied to the limb in different directions (Kalaska and Hyde 1985; Kalaska et al. 1989). Broad tuning is also characteristic of EMG activity during similar movement and isometric-force tasks (Buchanan et al. 1986; Buneo et al. 1997; Flanders and Soechting 1990; Hoffman and Strick 1999; Kakei et al. 1999; Kalaska et al. 1989).

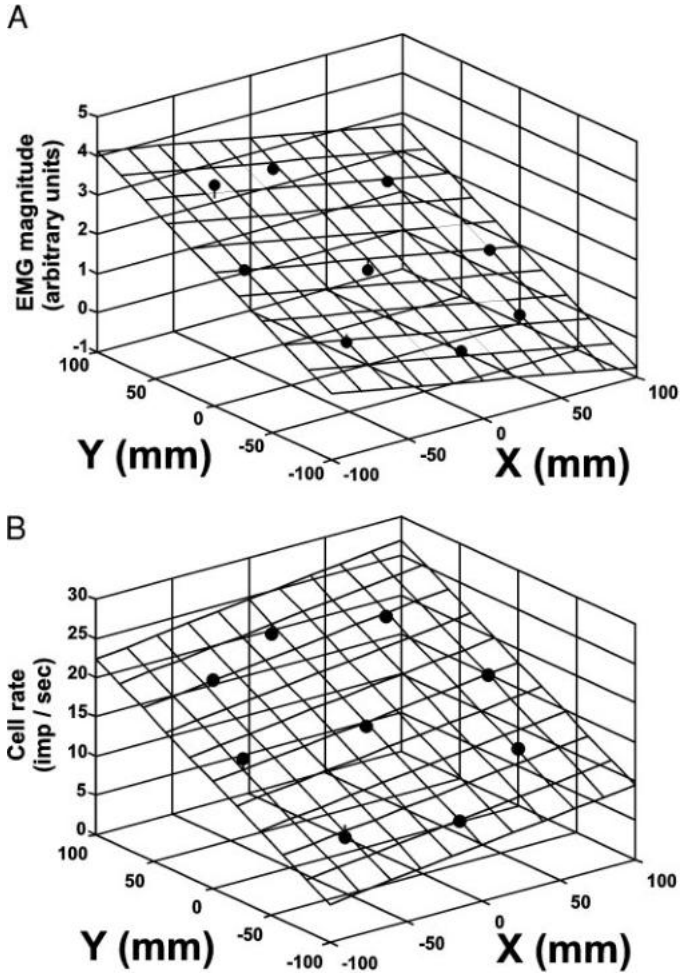

FIG. 10. *A*: mean activity of the right anterior deltoid of *monkey A* during THT at all hand locations (●) and its best-fit regression plane. *B*: mean activity of 1 left MI cell at all hand locations during THT and its best-fit regression plane.

The most salient finding of this study is that changes in arm posture had a powerful effect on MI cell activity, including changes in both discharge level and directional tuning, when monkeys used their whole arm to generate identical net isometric force ramps in different directions at the hand while holding the hand in different workspace locations. Cells typically showed planar changes in activity level as a function of hand location (i.e., arm posture) in a horizontal workspace. Changes in directional tuning varied systematically with hand location, resulting in a rotation of tuning at the single-cell and population levels about an approximately body-centered reference point. The cell response modulations could not be explained by systematic changes in output forces at different hand locations. Corresponding effects were observed for task-related muscle activity.

The second salient observation in this study was that arm posture-related effects on cell activity could be seen prior to (RT) and during (DFT) the generation of dynamic force output ramps of constant spatial directionality, as well as during the steady-state maintenance of isometric forces (THT). Furthermore, the strength of the posture-related effect was weaker during the RT epoch than later in the trial. This was especially evident for directional tuning. During the RT epoch, fewer cells showed a significant interaction between hand location and force direction (Table 2), overall directional tuning changes were smaller (Table 3*A*, Fig. 9), and fewer cells showed significant changes in directional tuning at different hand locations (Table 3*B*, Fig. 9).

Another salient finding was of directional and spatial anisotropy in the activity patterns. Arm location-dependent planar changes in overall activity tended to be inclined toward the body along an axis oriented away from the body midline toward the arm. The distribution of axes normal to the best-fit planes showed a mirror-image reversal for data collected in opposite hemispheres while the monkey used the arm contralateral to the recording site.

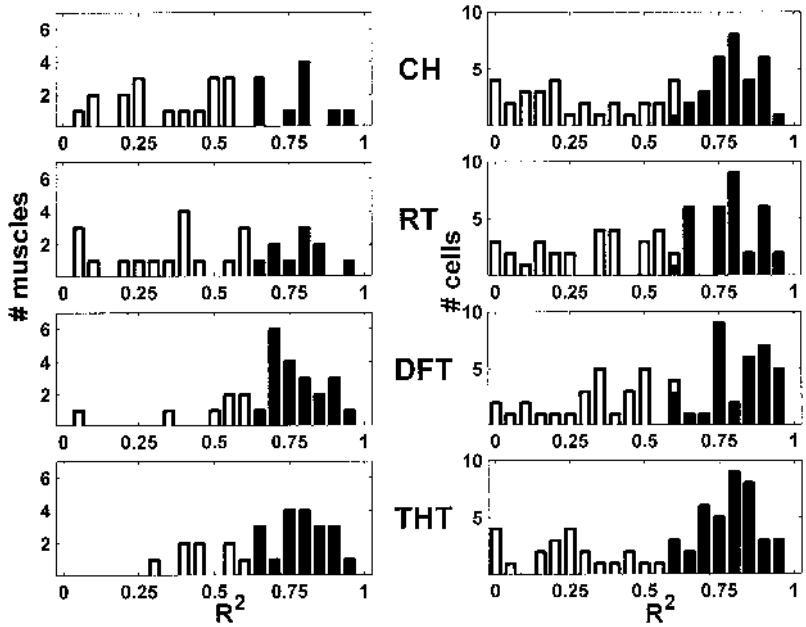

FIG. 11. Range of variance of mean activity of muscles (*left*, $n = 27$) and cells (*right*, $n = 61$) accounted for by a planar regression with *x*-*y* hand location. Cells and muscles having both significant (■) and nonsignificant planar fits (□) are shown.

TABLE 4. *Planar regression of cell and muscle activity on hand location: number of cells/muscles (percent) displaying activity fit by a significantly nonhorizontal regression plane ($P < 0.05$)*

Epoch	*n*	CHT	R^2	RT	R^2	DFT	R^2	THT	R^2
Cells	61	33 (54)	0.83	33 (54)	0.82	35 (57)	0.84	39 (64)	0.81
Muscles	27	10 (37)	0.8	12 (44)	0.82	20 (74)	0.81	20 (74)	0.82

R^2 value is mean R^2 of all cells having a significant regression ($P < 0.05$).

Effects of arm posture on directionality of cell activity in MI and PMd

DIRECTIONALITY. Caminiti et al. (1990, 1991) reported that the directional tuning of cell activity in MI and PMd rotated systematically about the vertical axis by an amount similar to the net rotation in shoulder angle about the same axis while reaching in the different horizontally distributed workspaces. Kakei et al. (1999) likewise reported that many MI cells showed systematic rotations of their directional tuning about the long axis of the forearm, when monkeys made isolated wrist movements in eight directions while holding the wrist in pronated, middle, or supinated postures. In contrast, Scott and Kalaska (Scott and Kalaska 1997; Scott et al. 1997) reported single-cell PD changes when monkeys made reaching movements along the same hand paths while holding the arm in two different postures but no evidence of a systematic rotation of the directional tuning of the entire sample population. They suggested that this was due to the geometry of their task in which the arm rotated about an axis parallel to the plane of movement. No net rotation of tuning functions would occur at the population level because the spatial tuning functions of different cells rotated into and out of the plane of action of the task (Scott and Kalaska 1997). In contrast, in the tasks used by Caminiti et al. (1990, 1991) and Kakei et al. (1999), the axis of rotation of the limb was perpendicular to at least one of the planes of motion.

The present study confirms this interpretation. When the limb posture changed about an axis perpendicular to the horizontal plane of motor output, there was a systematic rotation of MI tuning functions at both single-cell and population levels by an amount approximately equal to the changes in EMG tuning and the change in shoulder angle about the vertical axis. Furthermore, this change occurred in an isometric task that avoided complications introduced by the complex dynamics of arm movement.

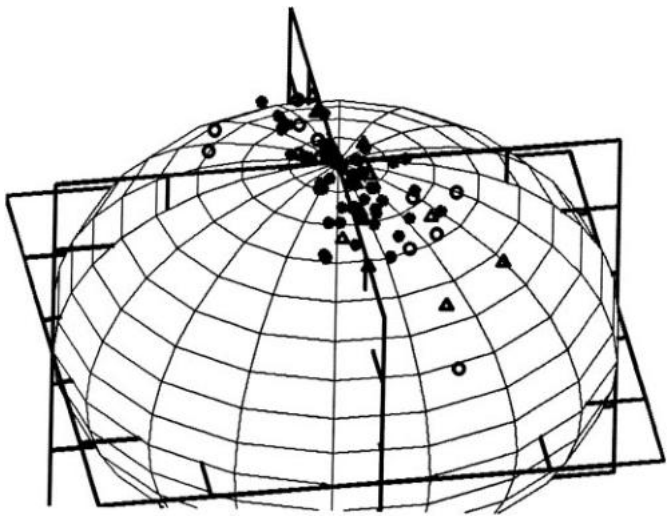

FIG. 12. Projection of vectors normal to best-fit planes for individual cells (○ and ●) and muscles (△ and ▲) onto the surface of a sphere. Left MI cells and right arm muscles: ● and ▲; right MI cells and left arm muscles: ○ and △. For graphic purposes, the data collected when the monkey used its left arm have been mirror-reflected about the mid-sagittal axis.

These posture-dependent changes in directional tuning and the way in which they are influenced by the geometry of different tasks is consistent with a role for MI in resolving the limb posture-dependent changes in the transformation between extrinsic spatial and intrinsic attributes of movement.

The results of Kakei et al. (1999) appear to suggest a smaller effect of posture on wrist-related MI activity than the studies using whole-arm tasks. However, this may be due mainly to methodological issues. First, quantitative analyses (ANOVA) revealed significant posture-related effects on most cells (Caminiti et al. 1990, 1991; Scott and Kalaska 1997; present study). Kakei et al. (1999) did not report the results of such an analysis. A more important factor, however, is the time period during which the data were analyzed. In Caminiti et al. (1990, 1991), Scott and Kalaska (1997), and the present study, posture-dependent effects were evaluated throughout the entire duration of each trial. In contrast, Kakei et al. (1999) limited their analysis to the last part of the RT epoch from 100 to 0 ms before movement onset. Posture-dependent directional effects were less prominent during the RT in the present study than later on in the trial. A similar trend was seen by Scott and Kalaska (1996). More strikingly, Kakei et al. (1999) reported that the distribution of direction changes was bimodal, suggesting the existence of two distinct groups of cells that were affected or not by postural changes before movement onset. Similar bimodal distributions of tuning changes were seen during the RT in the present study (Fig. 9*A*). This indicated substantial agreement between the two studies on the effect of limb posture on cell tuning functions in MI prior to motor output onset. Furthermore, the present results show that the bimodal distributions of PD shifts during RT were only prominent at lateral hand locations but not for locations close to the body midline and that they became much less prominent after the onset of the force ramps even at the lateral locations.

DIRECTIONAL CHANGES IN PRECENTRAL CORTEX: ARM POSTURE OR GAZE DIRECTION? Boussaoud et al. (Boussaoud and Bremmer 1999; Boussaoud et al. 1998; Jouffrais et al. 1999) have reported that the strength and directionality of arm movement-related cell activity in PMd is modulated by gaze direction and suggested that the directional shifts reported by Caminiti et al. (1990, 1991) might be due in part or entirely to the gaze shifts that occurred while the monkey made arm movements in the three adjacent target cubes. However, Scott and Kalaska (Scott and Kalaska 1997; Scott et al. 1997) found that single-cell tuning in MI and PMd often changed while monkeys made arm movements to targets in the same spatial locations using two

different arm postures. In the present study, rotations of cell PDs occurred with hand location in the workspace that were of the same magnitude as that in Caminiti et al. (1990, 1991) at both single-cell and population levels even though the desired force targets and visual feedback of net force output were presented in the same positions on a fixed computer monitor, independent of hand location. Therefore global gaze shifts are not necessary to produce changes in single-cell tuning coupled to changes in arm posture during both reaching movements and isometric force generation. Arm posture changes alone are sufficient. This is consistent with modeling studies that proprioceptive feedback about arm posture can provide sufficient information to resolve the visuomotor transformations between extrinsic and intrinsic movement parameters (Baraduc et al. 2001; Burnod et al. 1999).

Finally, the gaze-related modulations (Boussaoud et al.1998) arose during lengthy periods of imposed gaze fixation. In contrast, no gaze control was imposed in Caminiti et al. (1990, 1991), Scott and Kalaska (1997) or in the present study, and the monkeys were free to adopt whatever oculomotor strategy they wished. The impact of gaze direction on arm-related activity in the precentral gyrus during free gaze has yet to be fully evaluated (Cisek and Kalaska 2002).

Changes in response intensity

Many MI cells showed a systematic change in the level of task-related activity with arm posture that frequently took the form of a planar function of hand location. This was seen for both the overall grand mean of task-related activity across all directions of force output and for the activity related with each direction of force output. A smaller number of cells also showed a systematic planar change in the dynamic range of force direction-related changes in activity in different hand locations. Changes in the level of task-related activity independent of any directional changes represent another mechanism by which MI can contribute to the transformations required to compensate for posture-related changes in the coupling between extrinsic spatial and intrinsic movement parameters (Baraduc et al. 2001; Pouget and Sejnowski 1997; Salinas and Abbott 1995; Zipser and Andersen 1988).

Temporal gradient of posture-related discharge modulation

The effects of arm posture on MI activity, especially its directionality, were less prominent at the single-cell and population levels during RT than during DFT and THT. In particular, both Kakei et al. (1999) and the present study found evidence of the transient expression of a signal by a subset of cells in MI that appears to be coupled more closely to the extrinsic spatial attributes of the task than to the mechanics of its execution. A similar feature of MI activity has been found during the RT in many other studies (Georgopoulos et al. 1989, 1992; Scott and Kalaska 1996; Shen and Alexander 1997a,b; Taira et al. 1996; Zhang et al. 1997). The changes in the apparent coupling of MI activity to motor output parameters may also reflect the neuronal mechanisms that resolve the transformation from extrinsic to intrinsic reference frames (Johnson et al. 2001).

These findings are also consistent with evidence that the earliest part of the motor output signal is only an approximation of the exact motor command needed to successfully perform an action (Desmurget and Grafton 2000; Ghilardi et al. 1995; Gordon et al. 1994; Karst and Hasan 1991a,b; Massey et al. 1991; Soechting and Flanders 1989; Smyrnis et al. 2000). The existence of these early motor output errors has implications for the computational architecture of the motor system. It suggests that the motor system either does not attempt or is not capable of generating the perfect solution to the putative inverse kinematic and inverse dynamic transformations necessary to determine the correct muscle activity prior to initiation of the motor output. This could result from various sources of errors such as in estimation of initial arm position, target location, or limb dynamics. Peripheral feedback during generation of the isometric forces could help correct for these initial errors and cause the increased prominence of arm posture-related effects on cell activity seen between the RT and later trial epochs. Feedback signals could come from proprioceptors in the arm as well as visual inputs about cursor motion on the screen.

Of course, the initial output errors described in those studies do not necessarily reflect an absolute performance limit of the motor system. In most cases, the sole behavioral constraint related to endpoint accuracy with no control imposed on initial outputs. Likewise the postural effect in this study may have become more prominent after force output onset as behavioral constraints on force directionality became more critical. It would seem important practically and theoretically to devise experiments to define the limits on the accuracy of initial outputs.

Despite the potential role of feedback on these hand location effects, it is also clear that some cells showed significant directional shifts at different hand locations even prior to force ramp onset (Fig. 9*A*). This indicates that some MI cells can generate predictive feed-forward signals that can take arm geometry into account prior to motor onset to generate appropriate outgoing motor commands. Human behavioral studies suggest that this capacity of the motor system may result from adaptive "internal inverse models" of the biomechanical properties of the peripheral musculoskeletal system and of the mechanical properties of the environment with which it is interacting (Bhushan and Shadmehr 1999; Conditt et al. 1997; Flanagan and Lolley 2001; Flanagan and Wing 1997; Ghilardi et al. 1995; Jordan 1990; Kawato 1999; Krakhauer et al. 1999; Sabes 2000; Shadmehr and Mussa-Ivaldi 1994; Thoroughman and Shadmehr 1999; Wolpert and Gharamani 2000; Wolpert et al. 1995). Behavioral evidence further suggests that the computational elements of the internal models of task dynamics function in an intrinsic (joint- or muscle-centered) coordinate system (Bhushan and Shadmehr 1999; Krakhauer et al. 1999; Shadmehr and Moussavi 2000; Shadmehr and Mussa-Ivaldi 1994; Thoroughman and Shadmehr 1997). The presence of arm geometry-dependent directional shifts in MI during RT is consistent with this prediction from the behavioral evidence and would imply that MI receives signals from or even contributes to the putative internal inverse model for task dynamics.

Anisotropies of posture-related response modulations in MI

The net isometric force vectors generated at the hand were evenly distributed at 45° intervals around the circle and were of uniform length across all hand locations. Despite this uniformity of motor output, there were a number of nonuniform anisotropies in the patterns of MI activity at both the single-cell and population level that varied as a function of arm posture.

These nonuniformities likely reflect part of a central compensatory mechanism for the anisotropic mechanical properties of the limb. The limb tends to be stiffer along an axis between the hand and shoulder and more compliant along the orthogonal axis (Flash and Mussa-Ivaldi 1990; Mussa-Ivaldi et al. 1985). As a result, the spatial orientation of the stiffness ellipse changes systematically in an arc-like manner centered on the shoulder as the hand sweeps across the horizontal plane, and the degree of eccentricity of the stiffness ellipse decreases as the hand is held closer to the body (Flash and Mussa-Ivaldi 1990; Mussa-Ivaldi et al. 1985). Both of these trends were paralleled in this study by the patterns of anisotropies of MI activity. The PD shifts varied systematically with hand location in the same manner as the spatial orientations of the stiffness ellipses. Overall levels of discharge across force directions and the dynamic ranges of cell activity for different force directions tended to be greater when the arm was extended out away from the body even though the force levels were constant at all hand locations. These changes in activity level tended to vary in a planar fashion with hand location, and the orientations of the planes were nonuniform, tending to cluster along an axis that deviated away from the midline toward the shoulder of the arm being used to generate the forces. Finally, the anisotropic distributions of planes for cells in the two hemispheres were mirror inverted across the body midline, further supporting their relation to the geometry-dependent anisotropies of arm mechanics (Scott and Kalaska 1997). These effects could be seen to differing degrees at all times in the trial.

Limitations on interpretation

The cell sample in this study was drawn primarily from the caudal part of MI forming the bank of the central sulcus where previous studies have found that cells were more strongly modified by external loads and more unconditionally coupled to the execution of reaching movements than cells in more rostral parts of MI (Crammond and Kalaska 1996, 2000; Kalaska et al. 1989). Every attempt was made to record from cells across all cortical layers that met the basic criteria of a relationship to proximal-arm movement and directional tuning. We did not reject cells that showed little modulation of activity at different hand locations. Indeed, many of the cells were initially isolated and studied in an arm-movement task (Sergio and Kalaska 1998) before evaluating their activity in the isometric task. However, because of the requirement to isolate cells for long periods of time while testing them sequentially at different hand locations, there was an inevitable bias toward a greater probability of successful testing of all nine hand locations for the larger cells concentrated in intermediate layers of MI. The properties of cells with only partial data sets, including cells located outside of the large-cell layer, did not appear to be significantly different from those cells with complete data sets. Nevertheless it must be acknowledged that cell populations located in more rostral parts of MI or in the superficial layers of the cortex within the central sulcus may behave differently from the sample described here.

This study shows a number of parallels between some properties of the sampled MI cell activity, muscle activity, and limb mechanics. This does not imply, however, that all MI cells represent movement in a muscle-centered coordinate system or generate signals that exclusively and explicitly represent forces or muscle activity. For instance, whereas prime-mover muscles in this task typically showed ramp-like increases in activation during force generation (Fig. 5) (Sergio and Kalaska 1998), many MI cells showed an initial phasic response component that did not correlate with any initial component of the time profile of force output or EMG activation (Fig. 6) (Sergio and Kalaska 1998). Furthermore the findings in this study do not preclude the existence in MI of representations of higher-order aspects of movement planning independent of causal task dynamics and muscle activity. The findings do, however, provide further compelling support for the hypothesis that the primary motor cortex is implicated in the transformation from a more abstract or global representation to a more causal representation of motor outputs (Scott and Kalaska 1997; Shen and Alexander 1997a,b; Zhang et al. 1997).

We thank L. Girard for expert technical assistance. C. Leger (Département de Mathématiques et Statistiques, Université de Montréal) suggested the bootstrap test for significant changes in directional tuning as a function of hand location. G. Richard built the task apparatus. R. Albert, S. Dupuis, É. Clément, C. Valiquette, and J. Jodoin provided software and electronics support.

This study was supported by the Medical Research Council/Canadian Institute of Health Research (CIHR) Group Grant in Neurological Sciences (GR-15176) and a CIHR operating grant (MT-14519) (J. F. Kalaska), and by postdoctoral fellowships from the Fonds de la Recherche en Santé de Québec and the Fonds pour la Formation de Chercheurs et l'Aide à la Recherche Groupe de Recherche sur le Système Nerveux Central (L. E. Sergio).

Present address of L. E. Sergio: School of Kinesiology and Health Science, 350 Bethune College, York University, 4700 Keele Str., Toronto, Ontario M3J 1P3, Canada (E-mail: lsergio@yorku.ca).

REFERENCES

Ajemian R, Bullock D, and Grossberg S. Kinematic coordinates in which motor cortical cells encode movement direction. *J Neurophysiol* 84: 2191–2203, 2000.

Ashe J. Force and the motor cortex. *Behav Brain Res.* 87: 255–269, 1997.

Baraduc P, Guigon E, and Burnod Y. Recoding arm position to learn visuomotor transformations. *Cereb Cortex* 11: 906–917, 2001.

Bhushan N and Shadmehr R. Computational nature of human adaptive control during learning of reaching movements in force fields. *Biol Cybern* 81: 39–60, 1999.

Boussaoud D, Jouffrais C, and Bremmer F. Eye position effects on the neural activity of dorsal premotor cortex in the macaque monkey. *J Neurophysiol* 80: 1132–1150, 1998.

Boussaoud D and Bremmer F. Gaze effects in the cerebral cortex: reference frames for space coding and action. *Exp Brain Res* 128: 170–180, 1999.

Buchanan TS, Almdale DPJ, Lewis JL, and Rymer WZ. Characteristics of synergic relations during isometric contractions of human elbow muscles. *J Neurophysiol* 56: 1225–1241, 1986.

Buneo CA, Soechting JF, and Flanders M. Postural dependence of muscle actions: implications for neural control. *J Neurosci* 17: 2128–2142, 1997.

Burnod Y, Baraduc P, Battaglia-Mayer A, Guigon E, Koechlin E, Ferraina S, Lacquaniti F, and Caminiti R. Parieto-frontal coding of reaching: an integrated framework. *Exp Brain Res* 129: 325–346, 1999.

Cabel DW, Cisek P, and Scott SH. Neural activity in primary motor cortex related to mechanical loads applied to the shoulder and elbow during a postural task. *J Neurophysiol* 86: 2102–2108, 2001.

Caminiti R, Johnson PB, Galli C, Ferraina S, and Burnod Y. Making arm movements within different parts of space: the premotor and motor cortical

representation of a coordinate system for reaching to visual targets. *J Neurosci* 11: 1182–1197, 1991.

Caminiti R, Johnson PB, and Urbano A. Making arm movements within different parts of space: dynamic aspects in the primate motor cortex. *J Neurosci* 10: 2039–2058, 1990.

Cisek P and Kalaska JF. Modest gaze-related discharge modulation in monkey dorsal premotor cortex during a reaching task performed with free fixation. *J Neurophysiol* 88: 1064–172, 2002.

Conditt MA, Gandolfo F, and Mussa-Ivaldi FA. The motor system does not learn the dynamics of the arm by rote memorization of past experience. *J Neurophysiol* 78: 554–560, 1997.

Crammond DJ and Kalaska JF. Differential relation of discharge in primary motor cortex and premotor cortex to movements versus actively maintained postures during a reaching task. *Exp Brain Res* 108: 45–61, 1996.

Crammond DJ and Kalaska JF. Prior information in motor and premotor cortex: activity during the delay period and effect on pre-movement activity. *J Neurophysiol* 84: 986–1005, 2000.

Desmurget M and Grafton S. Forward modeling allows feedback control for fast reaching movements. *Trends Cognit Sci* 1: 423–431, 2000.

Flanagan JR and Lolley S. The inertial anisotropy of the arm is accurately predicted during movement planning. *J Neurosci* 15: 1361–1369, 2001.

Flanagan JR and Wing AM. The role of internal models in motion planning and control: evidence from grip force adjustments during movements of hand-held loads. *J Neurosci* 17: 1519–1528, 1997.

Flanders M and Soechting JF. Arm muscle activation for static forces in three-dimensional space. *J Neurophysiol* 64: 1818–1837, 1990.

Flash T and Mussa-Ivaldi F. Human arm stiffness characteristics during the maintenance of posture. *Exp Brain Res* 82: 315–326, 1990.

Fromm C. Changes in steady state activity in motor cortex consistent with the length-tension relation of muscle. *Pfluegers Arch* 398: 318–323, 1983.

Georgopoulos AP, Ashe J, Smyrnis N, and Taira M. The motor cortex and the coding of force. *Science* 256: 1692–1695, 1992.

Georgopoulos AP, Caminiti R, Kalaska JF, and Massey JT. Spatial coding of movement: a hypothesis concerning the coding of movement direction by motor cortical populations. *Exp Brain Res Suppl* 7: 327–336, 1983.

Georgopoulos AP, Kettner RE, and Schwartz AB. Primate motor cortex and free arm movements to visual targets in three-dimensional space. II. Coding of the direction of arm movement by a neural population. *J Neurosci* 8: 2928–2937, 1988.

Georgopoulos AP, Lurito JT, Petrides M, Schwartz AB, and Massey JT. Mental rotation of the neuronal population vector. *Science* 243: 234–236, 1989.

Ghilardi MF, Gordon J, and Ghez C. Learning an visuomotor transformation in a local area of workspace produces directional biases in other areas. *J Neurophysiol* 73: 2535–2539, 1995.

Gordon J, Ghilardi MF, Cooper SE, and Ghez C. Accuracy of planar reaching movements. II. Systematic extent errors resulting from inertial anisotropy. *Exp Brain Res* 99: 112–130, 1994.

Hoffman DS, and Strick PL. Step-tracking movements of the wrist. IV: Muscle activity associated with movements in different directions. *J Neurophysiol* 81: 319–333, 1999.

Johnson MT, Mason CR, and Ebner TJ. Central processes for the multiparametric control of arm movements in primates. *Curr Opin Neurobiol* 11: 684–688, 2001.

Jordan MI. Motor learning and the degrees of freedom problem. In: *Attention and Performance. XIII. Motor Representation and Control,* edited by Jeannerod M. Hillside, NJ: Erlbaum, 1990, p. 796–836.

Jouffrais C and Boussaoud D. Neuronal activity related to eye-hand coordination in the primate premotor cortex. *Exp Brain Res* 128: 205–209, 1999.

Kakei S, Hoffman DS, and Strick PL. Muscle and movement representations in the primary motor cortex. *Science* 285: 2136–2139, 1999.

Kalaska JF, Cohen DA, Hyde ML, and Prud'Homme M. A comparison of movement direction-related versus load direction-related activity in primate motor cortex using a two-dimensional reaching task. *J Neurosci* 9: 2080–2102, 1989.

Kalaska JF and Hyde ML. Area 4 and area 5: differences between the load direction-dependent discharge variability of cells during active postural fixation. *Exp Brain Res* 59: 197–202, 1985.

Kalaska JF, Scott SH, Cisek P, and Sergio LE. Cortical control of reaching movements. *Curr Opin Neurobiol* 7: 849–859, 1997.

Kalaska JF, Sergio LE, and Cisek P. Cortical control of whole-arm motor tasks. In: *Sensory Guidance of Movement. Novartis Foundation Symposium.* New York: Wiley, 1998, vol. 218, p. 176–200.

Karst GM and Hasan Z. Initiation rules for planar two-joint arm movements: agonist selection for movements throughout the workspace. *J Neurophysiol* 66: 1579–1593, 1991a.

Karst GM and Hasan Z. Timing and magnitude of electromyographic activity for two-joint arm movements in different directions. *J Neurophysiol* 66: 1594–1604, 1991b.

Kawato M. Internal models for motor control and trajectory planning. *Curr Opin Neurobiol* 9: 718–727, 1999.

Krakhauer JW, Ghilardi MF, and Ghez C. Independent learning of internal models for kinematic and dynamic control of reaching. *Nat Neurosci* 2: 1026–1031, 1999.

Mardia KV. *Statistics of Directional Data.* London: Academic, 1972.

Massey JT, Drake RA, and Georgopoulos AP. Cognitive spatial-motor processes. IV. Specification of the direction of visually guided isometric forces in two-dimensional space: information transmitted and effects of visual force-feedback. *Exp Brain Res* 83: 439–445, 1991.

Moran DW and Schwartz AB. Motor cortical activity during drawing movements: population representation during spiral tracing. *J Neurophysiol* 82: 2693–2704, 1999a.

Moran DW and Schwartz AB. Motor cortical representation of speed and direction during reaching. *J Neurophysiol* 82: 2676–2692, 1999b.

Mussa-Ivaldi FA, Hogan N, and Bizzi E. Neural, mechanical, and geometric factors subserving arm posture in humans. *J Neurosci* 5: 2732–2743, 1985.

Pouget A and Sejnowski TJ. Spatial transformation in the parietal cortex using basis functions. *J Cognit Neurosci* 9: 222–237, 1997.

Ramsay JO and Silverman BW. *Functional Data Analysis.* New York: Springer-Verlag, 1997.

Sabes PN. The planning and control of reaching movements. *Curr Opin Neurobiol* 10: 740–746, 2000.

Salinas E and Abbott L. Transfer of coded information from sensory to motor networks. *J Neurosci* 15: 6461–6464, 1995.

Schwartz AB, Kettner RE, and Georgopoulos AP. Primate motor cortex and free arm movements to visual targets in three-dimensional space. I. Relations between single cell discharge and direction of movement. *J Neurosci* 8: 2913–2927, 1988.

Schwartz AB. Motor cortical activity during drawing movements: single-unit activity during sinusoid tracing. *J Neurophysiol* 68: 528–541, 1992.

Scott SH, Gribble PL, Graham KM, and Cabel DW. Dissociation between hand motion and population vectors from neural activity in motor cortex. *Nature* 413: 161–165, 2001.

Scott SH and Kalaska JF. Temporal changes in the effect of arm orientation on directional tuning of cells in monkey primary motor (M1) and dorsal premotor (PMd) cortex during reaching. *Soc Neurosci Abstr* 22: 1829, 1996.

Scott SH and Kalaska JF. Reaching movements with similar hand paths but different arm orientations. I. Activity of individual cells in motor cortex. *J Neurophysiol* 77: 826–853, 1997.

Scott SH, Sergio LE, and Kalaska JF. Reaching movements with similar hand paths but different arm orientations. II. Activity of individual cells in dorsal premotor cortex and parietal area 5. *J Neurophysiol* 78: 2413–2426, 1997.

Sergio LE and Kalaska JF. Systematic changes in directional tuning of motor cortex cell activity with hand location while generating static isometric forces in constant spatial directions. *J Neurophysiol* 78: 1170–1174, 1997a.

Sergio LE and Kalaska JF. The effect of arm posture on MI cell discharge during isometric force generation in constant spatial directions. *Soc Neurosci Abstr* 23: 607.2, 1997b.

Sergio LE and Kalaska JF. Changes in the temporal pattern of primary motor cortex activity in a directional isometric force versus limb movement task. *J Neurophysiol* 80: 1577–1583, 1998.

Shadmehr R and Moussavi ZMK. Spatial generalization from learning dynamics of reaching movements. *J Neurosci* 20: 7807–7815, 2000.

Shadmehr R and Mussa-Ivaldi FA. Adaptive representation of dynamics during learning of a motor task. *J Neurosci* 14: 3208–3224, 1994.

Shen L and Alexander GE. Preferential representation of instructed target location versus limb trajectory in dorsal premotor area. *J Neurophysiol* 77: 1195–1212, 1997a.

Shen L and Alexander GE. Neural correlates of a spatial sensory-to-motor transformation in primary motor cortex. *J Neurophysiol* 77: 1171–1194, 1997b.

Smyrnis N, Gourtzelidis P, and Evdokimidis I. A systematic error in 2-D arm movements increases with increasing delay between visual target presentation and movement execution. *Exp Brain Res* 131: 111–120, 2000.

Soechting JF and Flanders M. Sensorimotor representations for pointing to targets in three-dimensional space. *J Neurophysiol* 62: 582–594, 1989.

Taira M, Boline J, Smyrnis N, Georgopoulos AP, and Ashe J. On the relations between single cell activity in the motor cortex and the direction and magnitude of three-dimensional static isometric force. *Exp Brain Res* 109: 367–376, 1996.

Thoroughman KA and Shadmehr R. Electromyographic correlates of learning an internal model of reaching movements. *J Neurosci* 19: 8573–88, 1999.

Todorov E. Direct cortical control of muscle activation in voluntary arm movements: a model. *Nat Neurosci* 3: 391–398, 2000.

Van Zuylen EJ, Gielen CCAM, and Denier van der Gon JJ. Coordination and inhomogeneous activation of human arm muscles during isometric torques. *J Neurophysiol* 60: 1523–1548, 1988.

Wadman WJ, Denier van der Gon JJ, and Derksen RJ. Muscle activation patterns for fast goal-directed arm movements. *J Hum Mov Stud* 6: 19–37, 1980.

Winters JM and Woo S. (Editors). *Multiple Muscle Systems: Biomechanics and Movement Organization.* New York: Springer-Verlag, 1990.

Wolpert DM and Ghahramani Z. Computational principles of movement neuroscience. *Nat Neurosci* 3 *Suppl*: 1212–1217, 2000.

Wolpert DM, Ghahramani Z, and Jordan NI. An internal model for sensorimotor integration. *Science* 269: 1880–1882, 1995.

Zhang J, Riehle A, Requin J, and Kornblum S. Dynamics of single neuron activity in monkey primary motor cortex related to sensorimotor transformation. *J Neurosci* 17: 2227–2246, 1997.

Zipser D and Andersen RA. A back-propagation programmed network that simulates response properties of a subset of posterior parietal neurons. *Nature* 331: 679–684, 1988.